地 震 研 究 所 彙 報
Bull. Earthq. Res. Inst.
Univ. Tokyo
Vol. 75 (2000) pp. 57-77

The 1999 Chi-Chi, Taiwan Earthquake: A Subduction Zone Earthquake on Land

Tetsuzo SENO[1)], Kenshiro OTSUKI[2)] and Chao-Nan YANG[3)]

[1)] Earthquake Research Institute, University of Tokyo, Tokyo, Japan
[2)] Graduate school of Earth Sciences, Tohoku University, Sendai, Japan
[3)] Department of Geology, National Taiwan University, Taipei, Taiwan

Abstract

The Chi-Chi earthquake occurred at the thrust-décollement in the accretionary prism of a young collision zone in central Taiwan. This event is thus not different from a subduction zone earthquake if Taiwan were covered by the sea water. The surface ruptures were accompanied by little damage except for the collapse of buildings standing across the surface faults. The slip directions of the surface faults were mostly NW, which is consistent with the earthquake slip vector, but there were also many W-SW and N directed slips. At the northwest corner of the earthquake fault, significant uplifts and multiple thrusts in the river bed occurred.

These might all be related to the fact that the shallow portion of the earthquake fault cut the weak accretionary prism and the sediment on it. The uplifts at the northwestern corner imply an abnormal tsunami if the area were under the sea, thus suggesting a new factor for the mechanism of tsunami earthquakes: deformation of the sediment or weak accretionary prism at the lowest trench slope (Seno, 2000). The Chi-Chi earthquake might provide a unique chance to observe a subduction earthquake on land.

Key words: Chi-Chi earthquake, Taiwan, accretion, tsunami earthquake

1. Introduction

On Sept. 20, 1999, 17: 47 GST (Sept. 21, 1: 47 on local time), the Chi-Chi earthquake (M_s=7.7) occurred in central Taiwan. The event caused destructive damage. Even though it occurred on land, the features of various phenomena associated with the event, i.e., damage, slip directions, and uplifts along the surface faults, were somewhat different from those with earthquakes on land such as the 1995 M_s=7.2 Kobe earthquake. This may be related to the fact that the event occurred in a tectonic situation that was different from intraplate earthquakes. In this article, we first present a tectonic interpretation of this event. We then show phenomena associated with the event, and interpret them from the viewpoint of the pertinent tectonic situation. Finally, we discuss their implications.

2. Tectonic situation

Taiwan is located at the Eurasian plate (EU)-Philippine Sea plate (PH) boundary (Fig. 1). To the north of Taiwan, PH is subducting beneath EU along the Ryukyu

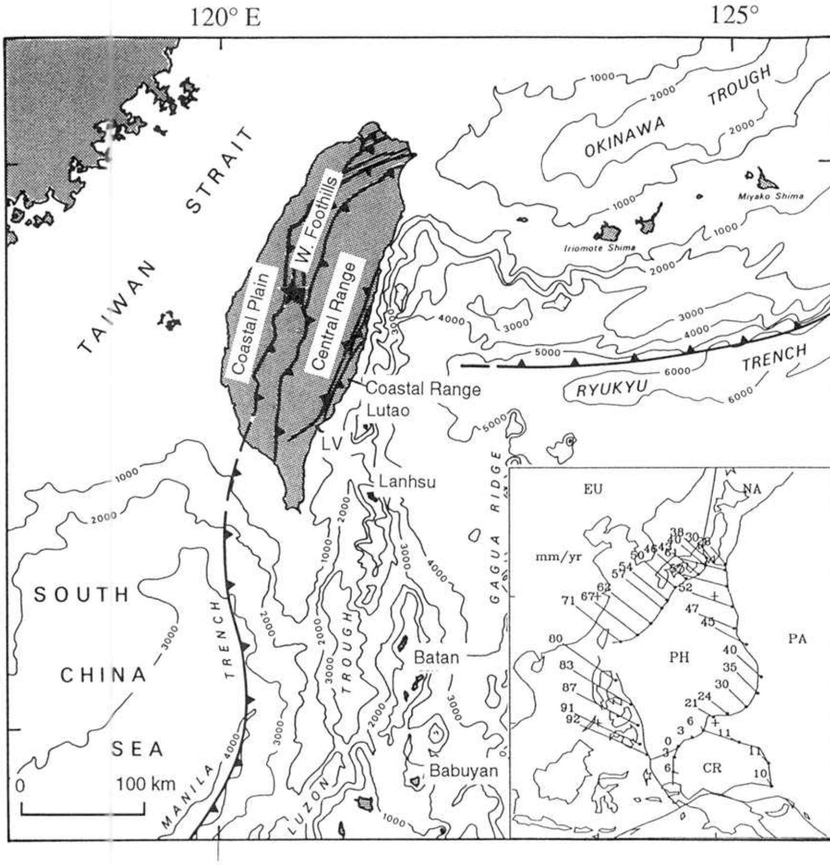

Fig. 1. Plate boundaries and tectonic elements in the vicinity of Taiwan (modified from Suppe, 1981). The motions of the Philippine Sea plate (PH) with respect to adjacent plates, Eurasia (EU), North America (NA), Pacific (PA), and Caroline (CA) plates (Seno *et al.*, 1993) are shown in the inset. LV denotes the Longitudinal Valley. The epicenter of the Chi-Chi earthquake (Central Weather Bureau) is shown by the star.

Trench, and to the south, EU, i.e., the South China Sea, is subducting beneath PH along the Manila Trench, forming the west-facing Luzon arc. Taiwan was originally at the continental shelf of the S.E. Asian margin, from which the South China Sea opened mainly in the Oligo-Miocene (Taylor and Hayes, 1980). The west-facing Luzon arc approached the margin and collided with the continental slope from 4 Ma (Suppe, 1981; Chi *et al.*, 1981), although the initial phases of the collision might have started as early as the middle Miocene (Teng, 1990). The sediment deposited at the continental margin during the Tertiary (Ho, 1986) has been offscraped and accreted to the Luzon arc due to the collision, and uplifted to form the west Central Range and the Western foothills (Suppe, 1981; 1985). The frontal thrust has advanced within the Coastal Plain, where the Quaternary sediment is deposited.

At present, the remnant Luzon volcanic arc is attached to the east coast of Taiwan as part of the Coastal Range (e.g., Chi *et al.*, 1981), which continues to the south as a remnant or active volcanic island chain, such as Lutao and Lanhsu, Batan and Babuyan islands. The Longitudinal Valley (LV) is a continuation of the North Luzon Trough, the forearc basin of the Luzon arc, morphologically. To the west of LV are the Central Range and the Western foothills. In the eastern part of the Central Range, high P/T metamorphosed crustal rocks are exposed (Jahn *et al.*, 1981), which can be interpreted as exhumation of the continental material once subducted (Lin and Roecker, 1998; Teng, 1990). Since we do not see any material originating from the Luzon arc west of LV, LV must be a suture zone of the collision, but the forearc material of the Luzon arc might be buried at depth beneath the Central Range.

Fig. 2 shows the W-E cross-section of central Taiwan (Seno, 1994) based on the geologic structures described above, with the geologic section of the Coastal Plain-Western foothills (Suppe, 1985). The structures shown in Fig. 2 are similar to the section in the Himalaya collision zone (e.g., Molnar, 1984); the foreland thrust belt is developed in front of the high mountains. However, the important difference is that in the Himalaya collision zone, the continental crust of the Indian plate has been offscraped and involved in the accretion; in contrast, in Taiwan the continental shelf-slope deposits are mainly involved in the accretion since the collision in Taiwan occurred much more recently.

The central one of the three thrusts shown in Fig. 2 is the Chelungpu fault at the surface, running along the western margin of the Western foothills. The surface ruptures of the Chi-Chi event appeared roughly along the Chelungpu fault, although at the northern end, it deviated significantly to the east from the geological fault. These thrusts, which cut the accretionary prism, are dipping to the east and merging into the décollement (Suppe, 1981, 1985). Some parts of the Chelungpu fault had been recognized as Quaternary active faults (Bonila, 1975; Ota and Okada, 1984; Ikeda, unpublished data, 1993).

The mainshock epicenter (Central Weather Bureau, Fig. 1) was located near the town of Chi-Chi east of the Chelungpu fault. The centroid depth and the SE dipping thrust-type focal mechanism solution (Harvard centroid moment tensor solution, HCMT) and the aftershock distribution determined by the temporary observation (Hirata *et al.*, 2000), compared to the geologic cross-section above, indicate that earthquake faulting occurred at the thrust, which dips to the east from the Chelungpu fault, and also along the décollement, and the hypocenter is located around the thrust-décollement intersection. The moment release pattern revealed by the teleseismic body wave analysis (Kikuchi *et al.*, 2000) showed a feature consistent with this, i.e., rupture initiated at the southern part of the fault plane, and propagated northward both to the shallower and deeper portions. The aftershock distribution, however, is more complicated; some aftershocks are apparently located below and above the décollement (See also Kao and Chen, 2000). This might be caused by the step-down of the décollement (See examples of such step-downs in Dahlen *et al.*, 1984).

The thrusts-décollement beneath the Western foothills and the west Central

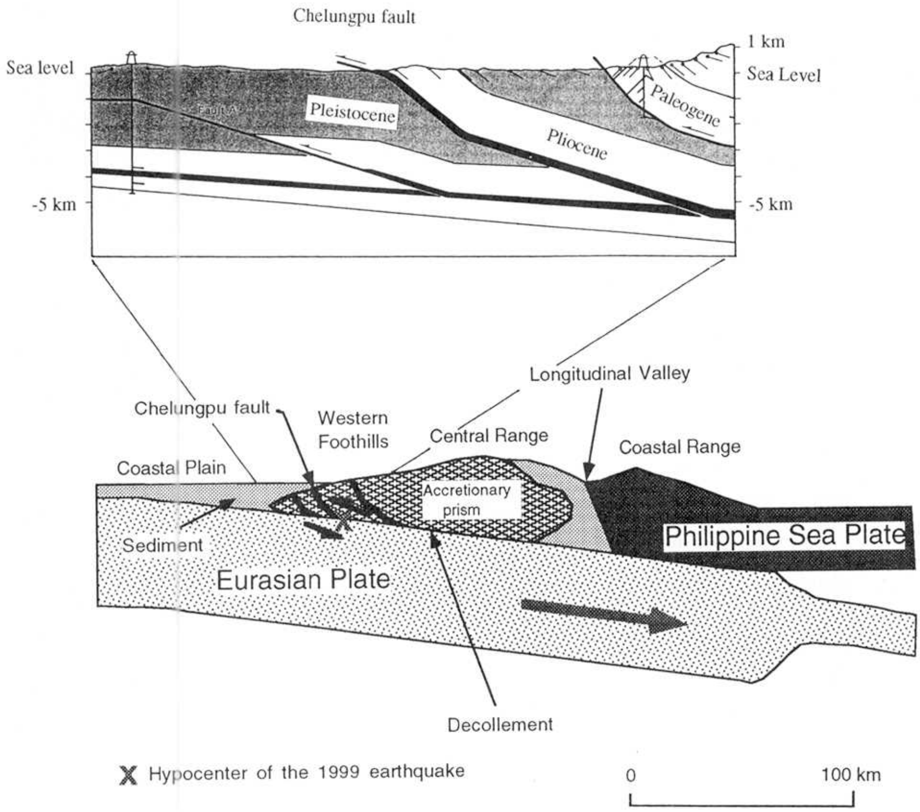

Fig. 2. Cross-section of central Taiwan. The upper figure shows the geological section constructed by Suppe (1985), which indicates the accretion of sediment at the Coastal Plain-Western foothills. The lower figure is modified from Seno (1994). The earthquake fault of the Chi-Chi event is probably covering the thrust and the décollement, which is the mechanical boundary between the Eurasian and Philippine Sea plates.

Range has been consuming the relative plate motion between EU and PH (Suppe, 1981; Seno, 1994), thus it constitutes a mechanical plate boundary. Seno (1994) estimated that a considerable portion of the relative motion is taken up along this boundary. Other fractions of the relative motion are consumed at LV and within PH off the east coast (Seno, 1994; Kao *et al.*, 2000). Since the Chi-Chi earthquake occurred at one of the mechanical plate boundaries, the event is regarded as an interplate earthquake. The slip vector of this event, N 55° W (HCMT), is almost coincident with the EU-PH motion (Seno *et al.*, 1993; Yu *et al.*, 1999a). Furthermore, because the event occurred at the thrust-decollement in the young accretionary prism, it is not different from an interplate thrust earthquake in the subduction zone, such as the 1946 Nankai earthquake at the Nankai Trough, southwest Japan.

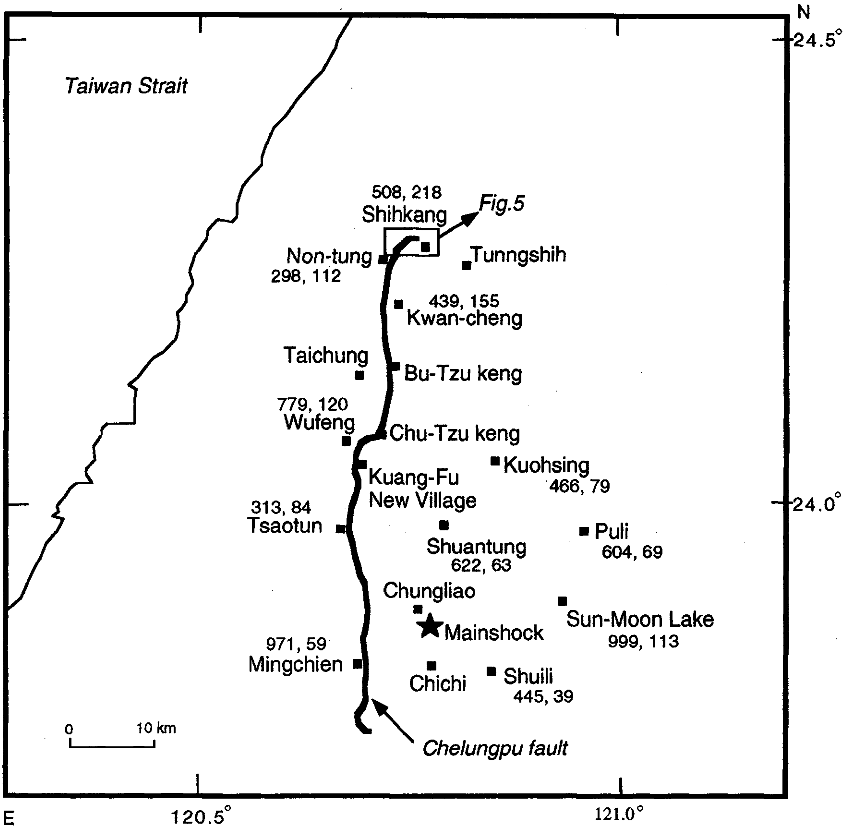

Fig. 3. Index map for the locations of towns. The surface fault trace along the Chelungpu fault (Central Geological Survey) is shown. The peak-to-peak values of maximum accelerations (unit: cm/s^2) and velocities (unit: cm/s) at strong motion sites are indicated (Lee *et al.*, 1999; Sakai *et al.*, 2000).

3. Phenomena associated with the 1999 Chi-Chi earthquake

As expected, the Chi-Chi earthquake showed somewhat different phenomena from inland earthquakes such as the 1995 Kobe earthquake. We describe these below and investigate the causes of these phenomena mainly from a tectonic viewpoint.

3.1 Damage

The severe damage caused by shaking due to strong motions generated by the event mainly occurred at local towns on the hanging wall such as the Sun-Moon Lake, Puli, Kuohsing, Chungliao, and Tungshih (e.g., Sakai *et al.*, 2000, See Fig. 3 for locations). In contrast, along the surface faults, little damage was seen except for collapsed buildings and houses, which just stood across the fault trace.

Photo 1 shows an example of damage along the surface fault, a factory in the town of Chu-Tzu Keng (See Fig. 3 for location). The right side of the factory was on the surface fault and was severely damaged (Photo 1 a). However, within the factory

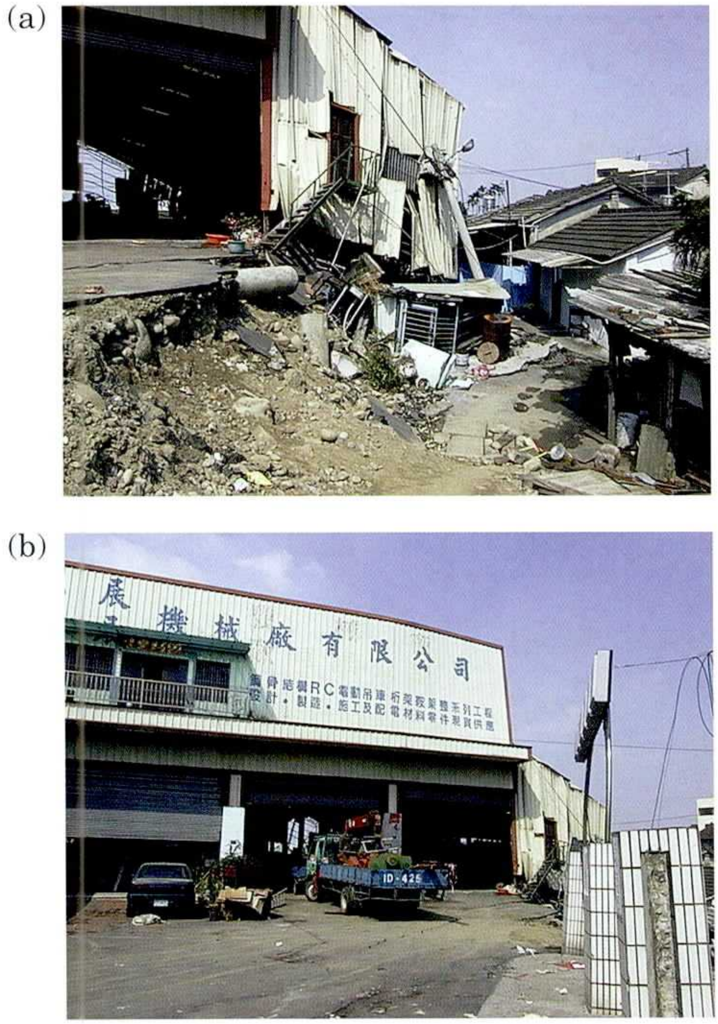

Photo 1. Factory in Chu-Tzu Keng (See Fig. 3 for location). (a) The right side of the factory was severely damaged and was standing over the surface fault, extending NE. (b) On the handing wall, in the rest of the factory, no damage was seen and the machines were running. The window glass was not broken.

on the hanging wall, a few meters from the surface fault, there was no damage; no window glass was broken, and the machines were running. Photo 2 shows another example in the town of Bu-Tzu Keng. The surface fault crossed the road, and passed between the two stores over the road (Photo 2 a). There was no damage to these stores. On the opposite side of the road, the building which stood across the fault had collapsed, but the stores on the hanging wall had little damage (Photo 2 b). In the northern corner of the surface faults, the fault scarp produced a fall in the Ta-Chia River (Photo 3). The surface fault passed between the pillars of the bridge and the

(a)

(b)

Photo 2. Stores in Bu-Tzu Keng (See Fig. 3 for location). The road was cut by the surface fault in the NE direction. (a) The road has a slope due to the fault scarp. The fault runs between the store with a white wall and that with a brown wall. There was no damage to these stores, and window glass was not broken. On the opposite side of the road, the building over the surface fault was severely damaged and tilted. (b) The view from the opposite side of Photo 2a. The tilted building is the one to the right in Photo 2a. The pillars of the stores on the hanging wall were slightly deformed.

bridge fell down; however, there was no damage to the buildings on the hanging wall seen in Photo 3.

These features were essentially seen along the whole length of the surface faults, except for some damage due to shaking in Wufeng and Shihkang (Sakai *et al.*, 2000), where the ground condition is bad. Photo 4a shows the fault scarp across a river in

Photo 3. Fall made of the surface fault in the Ta-Chia River (See Fig. 5 for location). The fault is striking NE, and the vertical offset is around 6 m (Otsuki and Yang, 1999). The buildings on the hanging wall had no damage.

the town of Chu-Tzu Keng, located about 100 m southwest of the location of Photo 1. The gravel on the hanging wall did not show any jumping, which indicates that the acceleration was not large. These are in marked contrast with damage associated with the 1995 Kobe earthquake, where many buildings and houses collapsed in the vicinity of the surface fault.

In fact, the peak-to-peak values of the acceleration were not high, i.e., less than 500 gal for the strong motion stations along the surface faults (Fig. 3, Lee *et al.*, 1999; Sakai *et al.*, 2000), except for Wufeng and Mingchien, the former of which had poor ground conditions and the latter had a malfunction of the strong motion seismometer. More specifically, Sakai *et al.* (2000) noted that the spectral components of the strong motion around 1 sec are critical for damage to low-rise buildings, and they were high for the stations on the hanging wall far from the surface faults, and resulted in collapse due to shaking of many buildings on the hanging wall; however, they were not high in areas along the surface faults. One reason for the low level of the strong motions around 1 sec period is the existence of large asperities of the Chi-Chi event in the northern part of the earthquake fault (Kikuchi *et al.*, 2000), which made the characteristic period of the faulting much longer than 1 sec.

However, the asperity size does not provide sufficient reason for the low level of the shorter period components of the strong motions. Note that even if the asperity size was small for the southern half of the earthquake fault (Kikuchi *et al.*, 2000), the feature of little damage along the surface faults due to shaking was the same for the southern part. If earthquake faulting is associated with stress drops at the shallow portion of the fault, the irregularities of the surface fault trace, multiple thrusts, and

(a)

(b)

Photo 4. Surface fault cut the river in Chu-Tzu Keng. This location is about 100 m southwest of that of Photo 1. The fault is striking NE. The uplifted hanging wall produced a depression behind it, forming a pond. No gravel jumped on the hanging wall.

stopping at the northern part of the earthquake fault inevitably would have produced strong motions at the shorter periods even if the asperity size was large.

The alternative mechanism we invoke is that a slip with a very low stress drop occurred along the shallow portion of the earthquake fault. It is noted that the shallow portion of the fault is along the thrust within the accretionary prism. It is generally known that the mechanical strength of accretionary prisms in subduction zones is very small within about 50 kilometers of the trench axis, avoiding seismic events (Byrne *et al.*, 1988). The high pore pressure amounting to 70% of the

Photo 5. Fault scarp in the peach farm northeast of the fall (See Fig. 5 for location). The original scarp was destroyed and formed a wide, gentle slope of large gravel. The vertical offset is around 6 m (Otsuki and Yang, 1999). There was no jumping of gravel and no damage to the two small cottages on the hanging wall.

Photo 6. Dam destruction looked from the north (See Fig. 5 for location). The vertical offset is around 9 m (Otsuki and Yang, 1999).

lithostatic pressure observed at the décollement west of the Chelungpu fault (Suppe, 1981) suggests that there might be free water along the thrusts, which would reduce the strength of the fault surface (See Moores, 1990 for examples of the existence of free water at the thrusts in the toe of the accretionary prism of the Nankai Trough). Thus it is reasonable to expect that there was low mechanical strength at the shallow portion of the Chi-Chi earthquake fault, which made the stress drop at the time of faulting very small. This does not contradict the fact that the peak-to-peak values of the velocity were high, especially for the northern stations along the surface faults (Fig. 3). Miyatake (personal comm., 2000) showed by numerical simulations that even if the shallow portion of an earthquake fault has a stress-free condition, faulting associated with that at the deeper asperities can have large slip velocities, but low acceleration.

3.2 Slip directions of the surface faults

Fig. 4 shows displacements along the surface faults measured by Otsuki and Yang (1999). Many of the slip vectors of the surface displacements are directed to NW, which is consistent with the earthquake slip vector (HCMT; Kikuchi *et al.*, 2000); however, there were also many W and SW directing slips in the measurements of Otsuki and Yang (1999). The most famous location with a slip differing from NW is that of the fault across the athletic ground of Kuang-Fu New Village. The measured direction was S74°W. In Fig. 4 there are five W and six SW slips. In addition, Sugiyama *et al.* (2000) measured three N slips in the northernmost area near Shihk-ang, and five SW and two W slips along the faults south of the Kuang-Fu New Village at different locations from Otsuki and Yang (1999).

This kind of anomalous slips associated with earthquakes may often be caused by landslides. Although landslides associated with the Chi-Chi event had occurred in the mountain area on the hanging wall, there is no evidence indicating landslides near the foot of the Western foothills. We believe that these anomalous slips were caused by the ductile behavior of the sediment pushed by the movement of the basement due to faulting. If the motion of the sediment was interrupted by any barriers, the sediment would have been squeezed in various ways like a liquid, resulting in ruptures with slips in various directions. This kind of ductile behavior would also be expected for inland intraplate reverse fault earthquakes when they cut a thick pile of sediment. However, it would generally be most common for subduction zone thrust earthquakes, which cut trench wedge sediment or sediment on an accretionary prism, although rupture directions might be obscured under the sea. For the Chi-Chi event, they seem to have become evident because it ruptured the margin of the Quaternary sedimentary basin of the Coastal Plain extensively at the surface.

3.3 Abnormal uplifts

At the northern corner of their surface faults, their strike changes from N-S to NE-SW and E-W, deviating from the geologically known Chelungpu fault. At this corner, the Ta-Chia River flows from east to west, forming an alluvial fan facing the Coastal Plain (Fig. 5). In the river bed, a fall in the river (Photo 3), a wide fault scarp made of gravel (Photo 5), and destruction of the dam wall (Photo 6) appeared. The coseismic uplifts of the hanging wall relative to the footwall at these sites are 6 m, 6 m, and 9 m, respectively (Otsuki and Yang, 1999). The large uplift of the dam wall might be affected partly by deformation of its long structural body, and we regard 6 m at the other two sites as the average uplift in the river bed south of the fault trace

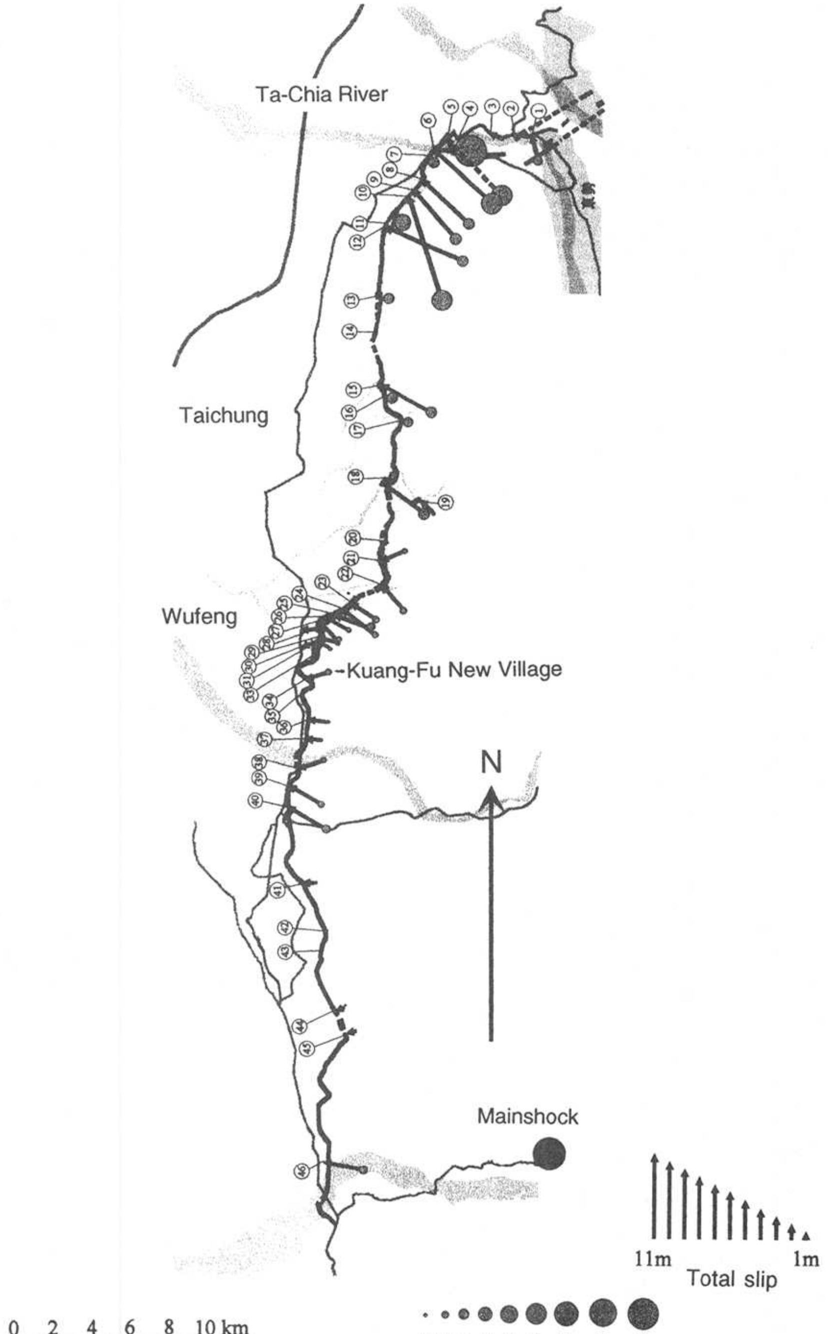

Fig. 4. Slip vectors and total amounts of the displacements of surface faults (arrows), and the vertical offsets (circles) (Otsuki and Yang, 1999).

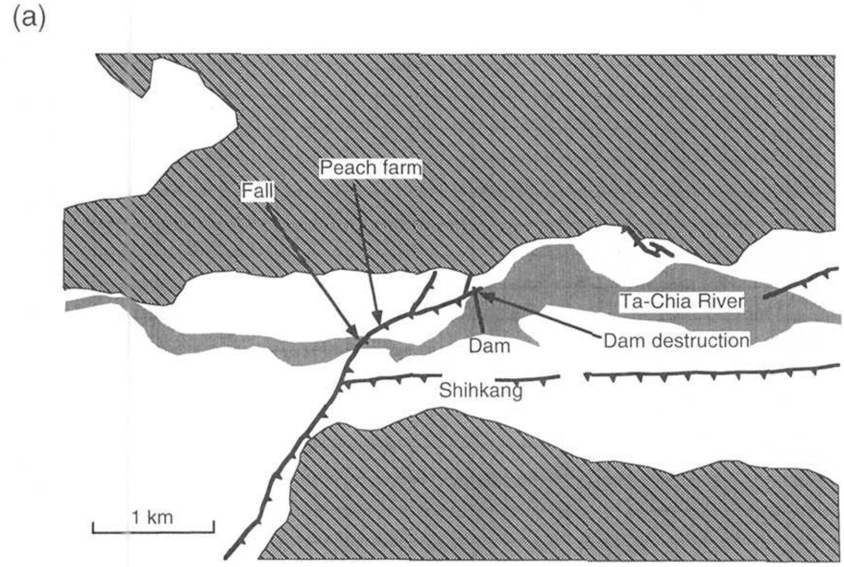

Fig. 5. Index map for the north end of the surface faults (Seno, 2000). In the river bed of the Ta-Chia River, the fall (Photo 3), gravel scarp in the peach farm (Photo 5), and dam destruction (Photo 6) occurred, and the thrusts became multiple. The fault trace is from the Central Geological Survey of Taiwan.

shown in Fig. 5.

The horizontal components of the coseismic displacements measured by GPS (Fig. 6, Yu *et al.*, 1999 b) are large in the northern part of the hanging wall south of the river, amounting to 7.1 m near Shihkang, than those in the southern part, which are around 3 m. In contrast, the vertical components of the coseismic displacements are nearly constant, i.e., around 3 m, everywhere in the hanging wall just east of the surface faults. Since the coseismic horizontal displacements northwest of the river is 0.7 m opposite the hanging wall side, there should be 7.8 m relative displacements between north and south of the Ta-Chia River. Since most of the GPS stations are established on the basement that consists of the accretionary prism, these displacements can be regarded as those of the basement. The overall distribution of the coseismic displacements revealed by GPS is consistent with the distribution of the seismic slips from an analysis of teleseismic long-period body waves (Kikuchi *et al.*, 2000). They are also consistent with ca. 7 m horizontal displacements of the surface faults at the northern corner (Otsuki and Yang, 1999).

However, the large uplifts in the river bed are not due to the large slips of the earthquake fault in the northwestern part, because a basement uplift of 3 m is expected from the elastic rebound of the 6 m's dip-slip (Kikuchi *et al.*, 2000) on the fault plane dipping at 30°, which is just the amount of the uplift maesured by GPS. Therefore, there is about a 3 m difference between the elastic uplift and the observed ones in the river bed, which implies that there were additional uplifts there.

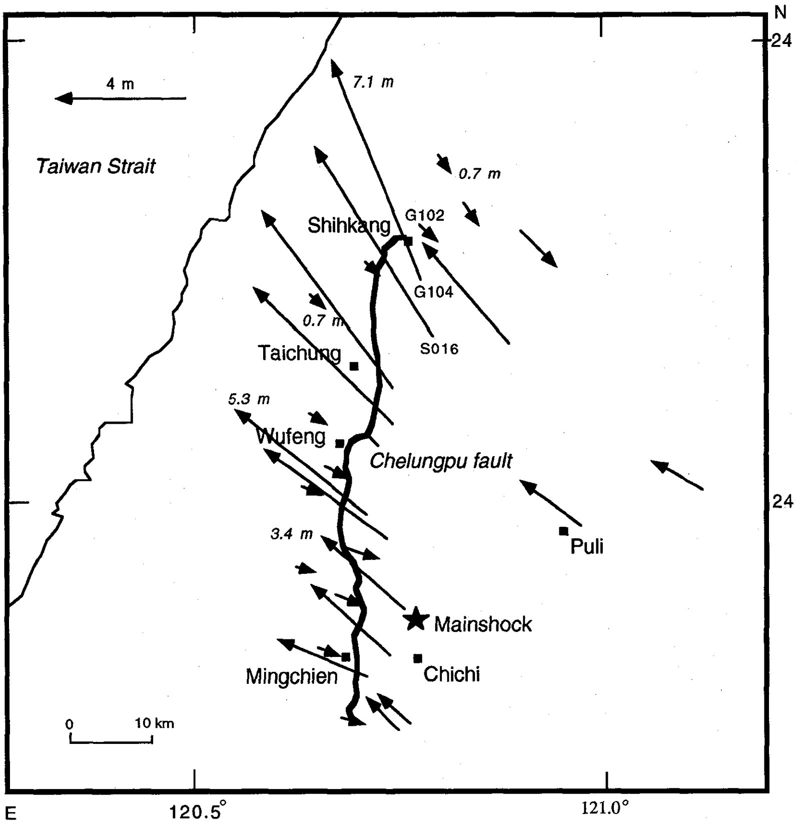

Fig. 6. Coseismic horizontal displacements associated with the Chi-Chi earthquake revealed by the GPS network (Yu *et al.*, 1999 b). Large displacements rotated clockwisely from the earthquake slip vector are seen in the northern portion of the hanging wall.

The hanging wall in the river bed consists of Pliocene sandstone and the sedimentary cover is thin. Note also that multiple thrusts appeared at the northwestern corner (Fig. 5). Seno (2000) applied the sand box experiment over the ductile décollement (Koyi *et al.*, 2000) to explain deformation at the northwestern corner. Koyi *et al.* (2000) demonstrated that the sand shortened above a ductile substrate shows multiple thrusts with simultaneous displacements (Fig. 7 b), while the sand above the frictional sheet shows a single thrust (Fig. 7 a). There was a large northward component of the faulting at the northwestern corner, as seen from the GPS horizontal movements, which implies that the slip at the northwestern corner is nearly horizontal. In addition, the shallowest portion of the earthquake fault at the northwestern corner is likely to have had very low friction, as seen from the high velocity of faulting recorded on the strong motion seismograms (Fig. 3, 1999). Therefore, the slip at the northwestern corner can be regarded as a slip on the ductile décollement, which would have produced the multiple thrusts and the associated

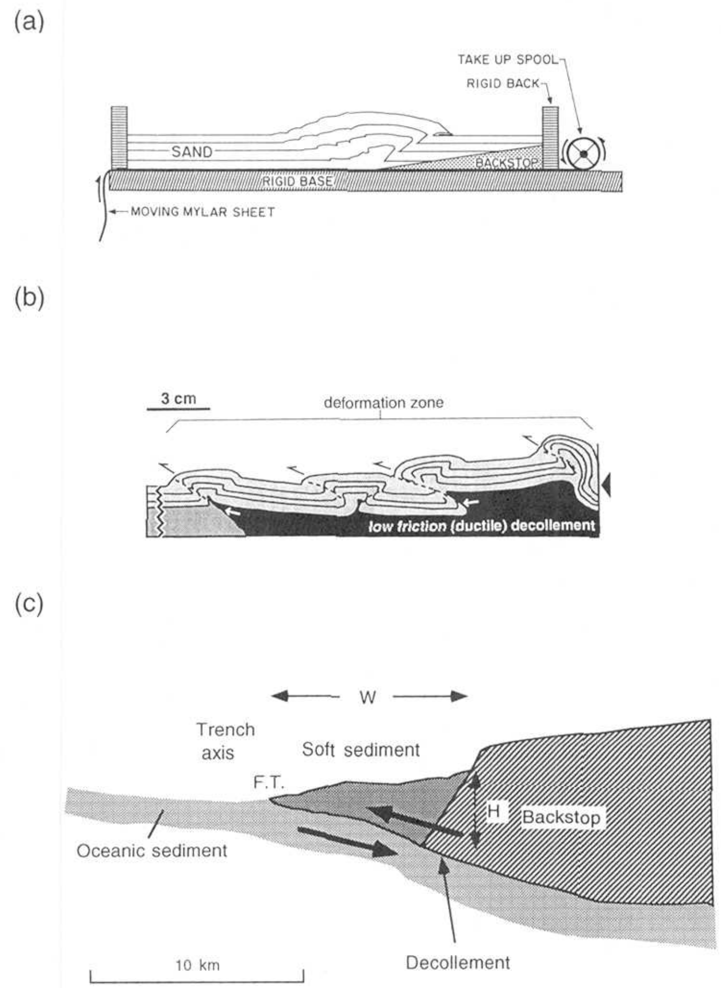

Fig. 7. (a) The uplift of sand due to the horizontal movement of the backstop (Byrne *et al.*, 1988). The mylar sheet is wound by the spool to the right, and the relative displacement between the sand and the backstop results in a single thrust. (b) The sand over the low-friction decollement (the Newtonian silicone polymer) is shortened, producing multiple thrusts (Koyi *et al.*, 2000). (c) A simplified cross-section of the Japan Trench (Seno, 2000; based on the section along 40°N by von Huene, 1986). In this section, the slump deposit is accumulated at the toe of the lower trench slope with the width of about 8 km, and the height of the backstop is about 4 km. *F.T. denotes the frontal thrust.*

uplifts.

4. Discussion

4.1 As a subduction zone earthquake

As shown in Section 2, the Chi-Chi earthquake ruptured the thrust-décollement of the accretionary prism of the young collision zone. Therefore, it is very similar to a subduction zone thrust type earthquake. The anomalous features of damage, slip directions, and uplifts along the surface faults can be understood from the viewpoint of a subduction zone earthquake.

The little damage along the surface faults except for the collapse of buildings which stood just across the faults might be related to the weakness of the shallow portion of the thrust. Much more detailed work should be conducted to understand the relationship between the damage, observed strong motions, and earthquake faulting, however. It might be important to take into account the effects of heterogeneous friction or material properties on the strong motions. The anomalous slip directions at the surface faults may be manifestation of the inelastic behavior of the sediment. The principle of active fault research is recovering earthquake faulting at depth from surface morphologic expressions. Although we admit that active fault studies are powerful tools for inland earthquakes, the Chi-Chi earthquake taught us that some caution is necessary. With a thick pile of sediment, fault traces may not cut the same position with every recurrence of earthquakes; morphologies and displacements accumulated by anomalous slips, such as the one in the athletic ground of the Kuang-Fu New Village, may not correspond to earthquake slip vectors.

In addition to the abnormal uplifts at the northwestern corner, the amounts of seismic slip and slip velocity were much larger in the northern part than in the southern part. This kind of heterogeneous distribution of slips associated with inland earthquakes is often found (Heaton, 1990; Ide and Takeo, 1997), which may be due to the heterogeneous distribution of fault strength, frictional properties, and tectonic stresses accumulated before the events. At present, however, the reason of the large slips is not known. Direct drilling of the fault plane of the Chi-Chi earthquake proposed by Ando *et al.* (2000) may help to elucidate some of the characteristics of the fault plane, such as the friction level, stress drop and a role of water along the fault plane. This earthquake provides a unique chance to conduct surveys of a zone similar to a seismogenic zone in a subduction zone from the land.

4.2 Implications for tsunami earthquakes

The abnormal uplifts at the northwestern corner, if it were under the sea, implies that tsunamis larger than those expected from the dislocation of the Chi-Chi earthquake have occurred. This has implications for the mechanism of tsunami earthquakes, although the expected tsunamis associated with the Chi-Chi event would have been minor due to the small area of the abnormal uplifts. Based on the uplifts at the northwestern corner, Seno (2000) proposed a new factor for the mechanism of tsunami earthquakes, i.e., sediment or weak accretionary prism at the toe of the inner trench slope is uplifted by the horizontal movement at the décollement. A possible example of the sediment deformation in the Japan Trench, where the 1896 $M_s=7.2$ Sanriku tsunami earthquake occurred, is shown in Fig. 7 c (Seno, 2000). In this two dimensional case, the uplift U_v is estimated by $U_v=dH/W$, where H is the vertical height of the backstop in the consolidated accretionary prism, W is the width of the uplifted area of the sediment, and d is the amount of dislocation. H is estimated to be

4 km and W is around 8 km in this section. Then about a 3 m uplift of the sedimentary wedge (slump deposit) can be expected by the dislocation of 6 m at the décollement. Tanioka and Seno (2000) showed that this amount of sediment uplift, with the basement uplift due to the elastic rebound, can successfully generate tsunamis associated with the 1896 Sanriku earthquake by numerical simulations. Without the sediment uplift, a dislocation of 10 m is necessary to explain the observed tsunamis.

The most popular mechanism so far proposed for tsunami earthquakes is a slow slip on the fault, which reduces the surface wave magnitude compared to the seismic moment (Kanamori, 1972; Pelayo and Wiens, 1992; Kanamori and Kikuchi, 1993). Although this mechanism seems to be applicable to almost all tsunami earthquakes, observed tsunamis are often larger than expected from the seismic moments derived from long-period seismograms (e.g., Fukao, 1979). There should therefore remain unknown factors for tsunami earthquakes (See also Kanamori and Kikuchi, 1993).

Fukao (1979) and Okal (1988) then proposed that a higher dip angle and the low rigidity in the weak accretionary prism can produce a larger uplift of the basement. Recent studies of tsunami earthquakes (Satake, 1994; Pelayo and Wiens, 1992; Johnson and Satake, 1997; Tanioka and Satake, 1996), however, do not support this. The fault planes revealed by these studies to explain the waveforms and arrival times of tsunamis extend very close to the trench axis, suggesting that faulting occurred on the basal décollement. Faulting on the décollement near the trench axis should have a very low dip angle, and would be inefficient for producing a large uplift of the basement. The enhanced displacement due to low rigidity is neither expected since the stress drop should be very small at the toe of the accretionary prism (Byrne *et al.*, 1988). We note that the new factor, i.e., deformation of the sediment or accretionary prism, is consistent with recent studies of tsunami earthquakes cited above, because deformation occurs due to a slip on the décollement at the lowermost trench slope. More detailed studies of the historical and instrument-recorded tsunami earthquakes are needed to demonstrate the proposed mechanism.

5. Conclusions

The 1999 Chi-Chi earthquake occurred at the thrust-décollement in the accretionary prism of a young collision zone in central Taiwan. This event is thus not different from a subduction zone earthquake if Taiwan were covered by the sea water. Damage due to shaking was concentrated at the towns on the hanging wall. In contrast, the surface ruptures were accompanied by little damage except for collapsed buildings, which stood just across the surface faults. The slip directions of the surface faults are mostly NW, consistent with the earthquake slip vector, but there are also many W-SW and N directed slips. Significant uplifts and multiple thrusts in the river bed occurred at the northwestern corner of the earthquake fault.

These might all be related to the fact that the shallow portion of the earthquake fault cut the weak accretionary prism and the sediment on it. The weakness of the shallow portion of the fault would have reduced damage due to shaking along the surface ruptures. The various directions of the slips may have been caused by the ductile behavior of the sediment. The abnormal uplifts and multiple thrusts at the northwestern corner may be explained by the slip on the ductile décollement. The uplifts imply an abnormal tsunami if the area were under the sea, thus suggest deformation of the sediment or weak accretionary prism at the lowermost trench slope as a new factor of the mechanism for tsunami earthquakes (Seno, 2000). The Chi-Chi earthquake, therefore, might provide a unique opportunity to observe a subduction zone earthquake on land.

Acknowledgements

We benefited from discussions with Yuan Wang and Wuu-Liang Huang during the field survey of the surface faults of the Chi-Chi event. We would like to express our thanks to Teruyuki Kato and Naoshi Hirata for their critical review of the manuscript, John Suppe for providing geologic cross-sections in central Taiwan, Yoshiko Yamanaka, Yuichiro Tanioka, Yoshio Fukao, Yuki Sakai, Yasutaka Ikeda, Mitsuhisa Watanabe, Teruo Yamashita, Takeshi Miyatake, Kenji Kanjo, Katsuhiko Ishibashi, and Naoshi Hirata for discussions, and Honn Kao, Msayuki Kikuchi, Yoko Ota, Yuichi Sugiyama, Kazuki Matsuura for preprints and Honn Kao for teaching us the local names of the study area.

References

ANDO, M., J. MORI, H. TANAKA, J.-H. HUNG and M. ZOBACK, 2000, Drilling the Chelungpu fault, Taiwan: Cores and heat-flow from a thrust-fault with very large displacements in a recent earthquake, A proposal to Science and Technology Agency, Jpn.

BONILA, M.G., 1975, A review of recently active faults in Taiwan, *U.S. Geol. Surv. Open File Rep.*, **75**, 41–58.

BYRNE, D.E., D.M. DAVIS and L.R. SYKES, 1988, Loci and maximum size of thrust earthquakes and the mechanics of the shallow region of subduction zones, *Tectonics*, **7**, 833–857.

CHI, W-R., J. NAMSON and J. SUPPE, 1981, Stratigraphic record of plate interactions in the Coastal Range of eastern Taiwan, *Mem. Geol. Soc. China*, **4**, 155–194.

DAHLEN, F.A., DAVIS, D. and J. SUPPE, 1984, Mechanics of fold-and-thrust belts and accretionary wedges: Cohesive Coulomb theory, *J. Geophys. Res.*, **89**, 10087–10101.

FUKAO, Y., 1979, Tsunami earthquakes and subduction processes near deep-sea trenches, *J. Geophys. Res.*, **84**, 2303–2314.

HEATON, T.H., 1990, Evidence for and implications of self-healing pulses of slip in earthquake rupture, *Phys. Earth Planet. Inter.*, **64**, 1–20.

HIRATA, N., S. SAKAI, Z.-S. LIAW, Y.-B. TSAI and S.-B. YU, 2000, Aftershock Observation of the 1999 Chi-Chi, Taiwan, Earthquake, Bull. Earthquake Res. Inst., this volume.

HO, C.S., 1986, A synthesis of the geologic evolution of Taiwan, *Tectonophysics*, **125**, 1–16.

IDE, S. and M. TAKEO, 1997, Determination of constitutive relations of fault slip based on seismic wave analysis, *J. Geophys. Res.*, **102**, 27379–27391.

JAHN, B.M., J.G. LIOU and H. NAGASAWA, 1981, High-pressure metamorphic rocks of Taiwan: REE geochemistry, Rb-Sr ages and tectonic implications, *Mem. Geol. Soc. China*, **4**, 497–520.

JOHNSON, J.M. and K. SATAKE, 1997, Estimation of seismic moment and slip distribution of the

April 1, 1946, Aleutian tsunami earthquake, *J. Geophys. Res.*, **102**, 11765–11774.

KANAMORI, H., 1972, Mechanism of tsunami earthquakes, Phys. Earth Planet. Interiors, **6**, 346–359.

KANAMORI, H. and M. KIKUCHI, 1993, The 1992 Nicaragua earthquake: a slow tsunami earthquake associated with subducted sediments, *Nature*, **361**, 714–716.

KAO, H, G-C. HUANG and C-S. LIU, 2000, Transition from oblique subduction to collision in the northern Luzon arc-Taiwan region: Constraints from bathymetry and seismic observations, *J. Geophys. Res.*, in press.

KAO, H. and CHEN, W.-P., 2000, The Chi-Chi earthquake sequence of September 20, 1999 in Taiwan: Seismotectonics of an active, out-of-sequence thrust, Science, in press.

KIKUCHI, M., Y. YAGI and Y. YAMANAKA, 2000, Source process of the Sept. 21 1999 Central Taiwan earthquake, Bull. Earthq. Res. Inst., Univ. of Tokyo, this volume.

KOYI, H.A., K. HESSAMI and A. TEIXELL, 2000, Epicenter distribution and magnitude of earthquakes in fold-thrust belts: insights from sandbox models, *Geophys. Res. Lett.*, **27**, 273–276.

LEE, W.H.K., T.C. SHIN, K.W. KUO and K.C. CHEN, 1999, CWB Free-Field Storng-Motion Data from the 921 Chi-Chi Earthquake: Volume 1. Digital Acceleration Files on CD-ROM, Seismology Center, Central Weather Beureau, Taipei, Taiwan.

LIN, C.H. and S.W. ROECKER, 1998, Active crustal subduction and exhumation in Taiwan, When Coninents Collide: Geodynamics and Geochemistery of Ultra High-pressure Rocks, edited by Hacker, B.R. and J.G. Liou, Kluwer Academic Publishers, 1998, 1–25.

MOLNAR, P., 1984, Structure and tectonics of the Himalaya: Constraints and implications of geophysical data, *Ann. Rev. Earth Planet Sci.*, **12**, 489–518.

MOORE, G.F., T.H. SHIPLEY, P.L. STOFFA, D.E. KARIG, A. TAIRA, S. KURAMOTO, H. TOKYUYAMA and K. SUEYHIRO, 1990, Structure of the Nankai Trough accretionary zone from multichannel seismic reflection data, *J. Geophys. Res.*, **95**, 8753–8765.

OKAL, E., 1988, Seismic parameters controlling far-field tsunami amplitudes: A review, *Natural Hazards*, **1**, 67–96.

OTA, Y. and A. OKADA, 1984, Active structures in Kyushu, Ryukyu islands, and Taiwan, Mobile belts in Asia, ed. by K. Hujita, Kaibundo, 147–177 (in Japanese).

OTSUKI, K. and C.-N. YANG, 1999, Surface displacements of the faults associated with the 1999 Chi-Chi earthquake, Rep. Grant-in-Aid for Scientific Research on the Taiwan earthquake, Sept. 20, 1999 (in Japanese).

PELAYO, A.M. and D.A. WIENS, 1992, Tsunami earthquakes: Slow thrust-faulting events in the accretinary wedge, *J. Geophys. Res.*, **97**, 15321–15337.

SAKAI, Y., K. KOKETSU, S. YOSHIOKA and T. KABEYASAWA, 2000, Damage to buildings caused by the 1999 Taiwan Chi-Chi earthquake and earthquake response analyses using recorded strong ground motions, Bull. Earthquake Res. Inst., this volume.

SATAKE, K., 1994, Mechanism of the 1992 Nicaragua tsunami earthquake, *Geophys. Res. Lett.*, **21**, 2519–2522.

SENO, T., 1994, Tectonics of the Taiwan region, *Jisin*, **46**, 461–477 (in Japanese).

SENO, T., 2000, The September. 21, 1999 Chi-Chi earthquake in Taiwan: implications for tsunami earthquakes, *Terr. Atmos. Ocean Sci.*, **11**, 701–708.

SENO, T., S. STEIN and A.E. GRIPP, 1993, A model for the motion of the Philippine Sea plate consistent with NUVEL-1 and geological data, *J. Geophys. Res.*, **89**, 17941–17948.

SUGIYAMA, Y., A. KARIYA and T. AZUMA, 2000, Surveys of the surface displacements of the faults associated with the Sept. 21 1999 Chi-Chi earthquake, Rep. Corrd. Comm. Earthquake Prediction, 63, in press (in Japanese).

SUPPE, J., 1981, Mechanics of mountain building and metamorphism in Taiwan, *Mem. Geol. Soc. China,* **4**, 67–89.

SUPPE, J., 1985, Principles of Structural Geology, Prentice-Hall Inc., N.J., 537 pp.

TANIOKA, Y. and K. SATAKE, 1996, Fault parameters of the 1896 Sanriku tsunami earthquake estimated from tsunami numerical modeling, *Geophys. Res. Lett.,* **23**, 1549–1552.

TANIOKA, Y. and T. SENO, 2000, The sediment deformation model for the 1896 Sanriku tsunami earthquake, Abstr. WPGM, 2000, Tokyo.

TAYLOR, B., D.E. and HAYES, 1980, The tectonic evolution of the south China Basin, *Geophys. Monog. AGU,* **23**, 89–104.

TENG, L.S., 1990, Geotectonic evolution of late Cenozoic arc-continent collision in Taiwan, *Tectonophysics,* **183**, 57–76.

VON HUENE, R., 1986, To accrete or not accrete, that is the question, *Geol. Rundsch.,* **75**, 1–15.

YU, S.-B., L.-C. KUO, R.S. PUNNNGBAYAN and E.G. RAMOS, 1999a, GPS observation of crustal deformation in the Taiwan-Luzon region, *Geophys. Res. Lett.,* **27**, 923–926.

YU, S.-B., L.C. KUO, Y.J. HSU, C.S. HOU, C.C. LIU, H.H. SU, J.F. LEE and T.C. LAI, 1999b, Coseismic and post-seismic deformations associated with the 1999 Chi-Chi earthquake, *Natural Sciences Newsletter,* NSC., **11**, 156–161.

(Received March 14, 2000)
(Accepted May 31, 2000)

The 1999 Chi-Chi, Taiwan Earthquake: A Subduction Zone Earthquake on Land

1999年台湾集集地震：陸上にのりあげた海溝系地震

瀬野徹三[1]・大槻憲四郎[2]・楊　昭雄[3]

[1] 東京大学地震研究所
[2] 東北大学理学系大学院
[3] 台湾大学地質研究所

1999年9月21日台湾中央部で起きた集集地震は，ルソン弧と中国大陸縁との間の衝突でできた付加体を切る逆断層（スラスト）で起きた．ここはユーラシアプレートとフィリピン海プレートとのプレート力学境界にあたり，通常の沈み込み帯でおきる地震と地学的には変わらない．地表で車籠埔断層として知られていた活断層に沿って地表断層が現れたが，その付近では，地表断層をまたいだ建物が壊れているのが特徴で，それ以外の被害は小さかった．地表断層のすべり方向は，かなりのものは北西方向であったが，一方西，南西，北方向のすべりもかなりの数がみられた．地表断層の北端では，大甲渓という河川の中の滝，桃畑の砂利断層崖，ダムの破損地などにおいて，弾性理論から期待できる隆起よりも3mほど大きい隆起が起きた．

これらの現象は，集集地震が本質的には海溝系の地震で，付加体中のスラストで起きたことと密接に関連していると考えられる．付加体浅部は力学的に大変弱く，大きな差応力を保持できない．したがって断層浅部の破壊強度は小さかったと考えられ，地震にともなう応力降下も小さかったであろう．これは，振動の周期が長かったことに加えて，地表断層付近の被害の特徴を説明するだろう．地表断層のいろいろな方向のすべりは，断層運動が表層付近で厚い堆積物を押し，押し出された堆積物がいろいろな方向にはみ出して，地表での断裂とすべりを生じたものと考えられる．北端の異常隆起は，ほぼ水平の断層面上のすべりによって付加体末端部に多重スラストが生じたためと考えられる．北端部の異常隆起は，もし海面下であれば異常津波を発生したことを意味しており，津波地震のメカニズムとして，海溝陸側斜面先端部の弱い付加体あるいは堆積物の変形が一因であることを示唆している．